World Academy of Science, Engineering and Technology
International Journal of Structural and Construction Engineering
Vol:17, No:6, 2023

Vibration Transmission across Junctions of Walls and Floors in an Apartment Building: An Experimental Investigation

Hugo Sampaio Libero, Max de Castro Magalhaes

***Abstract*—**The perception of sound radiated from a building floor is greatly influenced by the rooms in which it is immersed and by the position of both listener and source. The main question that remains unanswered is related to the influence of the source position on the sound power radiated by a complex wall-floor system in buildings. This research is concerned with the investigation of vibration transmission across walls and floors in buildings. It is primarily based on the determination of vibration reduction index via experimental tests. Knowledge of this parameter may help in predicting noise and vibration propagation in building components. First, the physical mechanisms involving vibration transmission across structural junctions is described. An experimental set-up is performed to aid this investigation. The experimental tests have showed that the vibration generation in the walls and floors are directed related to their size and boundary conditions. It is also shown that the vibration source position can affect the overall vibration spectrum significantly. Second, the characteristics of the noise spectra inside the rooms due to an impact source (tapping machine) are also presented. Conclusions are drawn for the general trend of vibration and noise spectrum of the structural components and rooms respectively. In summary, the aim of this paper is to investigate the vibro-acoustical behavior of building floors and walls under floor impact excitation. The impact excitation was at distinct positions on the slab. The analysis has highlighted the main physical characteristics of the vibration transmission mechanism.

***Keywords*—**Vibration transmission, Vibration Reduction Index, Impact excitation, building acoustics.

I. INTRODUCTION

THERE are many apartment buildings around the world that still do not comply with their current city council regulations on minimum sound insulation requirements. Many engineers have concentrated on analyzing structural response to a particular dynamic loading using uncoupled structural modes for the building components. In this case, the boundary condition at the interface between walls and floors, which is due to the velocity of the corresponding structure, cannot be replicated. Hence, the aim of this paper is to develop alternative in-situ test for the measurement of vibration transmission. It is performed here initially to structural coupled components in order to verify the accuracy and applicability of the approach.

Recently, various researchers [5]-[8] have concentrated their work on presenting the main advantages of floating floors in terms of their sound isolation effectiveness. The use of floating floors on building construction is well-known among civil engineers, architects and acoustic space designers. They are popular not only for their ability to decrease the transmission of structure-borne sound throughout the building structural components but also for their slender dimension which may be relevant on the calculation of the building total cost price.

Although the physical understanding of floating floor mechanisms is well established, the assessment of the sound power radiated by the structural floor has not been fully considered in terms of its boundary conditions. For example, it is important to know the relationship between the vibration transmission across wall-floor junctions and the sound pressure inside the adjacent rooms. Recently some researchers [5]-[8] have concentrated their investigation on optimizing the dynamic models of floating floor systems in order to improve their effectiveness, i.e., to minimize the transmitted vibrational energy to the structural floor.

The effects of panel boundaries on sound radiation, including a comparison with an infinite panel have been discussed by several researchers [1]-[3]. A simple two-dimensional model has been used for evaluating the sound radiation characteristics of finite panels [3]. The analysis of the radiation, through a baffled plate of finite width and infinite length, was rigorously performed. The effects of panel size have been studied in frequency regions below, above and at the critical frequency. In addition, estimates of averaged response over a given frequency range have also been investigated. The literature survey has revealed that a significant amount of work has concentrated on analyzing sound radiation of simply supported panels [5]-[8].

This research was undertaken as a result of the need to develop an easy and reliable methodology for measuring the floor-wall vibration transmission in order to obtain better comprehension of structure-borne vibration transmission across an apartment slab.

II. EXPERIMENTAL TESTS

The vibration transmission experiments were performed in a particular unreinforced masonry building. The building is composed of four floors. Each structural floor and load bearing wall has a thickness equal to 10 cm and 15 cm respectively. The tests were made on the 2nd floor of a particular apartment. The external noise influences were well below the vibration level measurements in the walls and floors, i.e., the signal-to-noise

Hugo S Libero is with Electrical Engineering Department, Universidade Federal de Goiás, Av. Antonio Carlos 6627, 31270-901, Belo Belo Horizonte, Brazil

Max de Castro Magalhaes is with Structural Engineering Department, Universidade Federal de Minas Gerais, Av. Antonio Carlos 6627, 31270-901, Belo Belo Horizonte, Brazil (e-mail: maxdcm@gmail.com).

ratio was high enough to assure good quality measurements. The experimental set-up and floor characteristics are shown in Figs. 1 and 2. First, a tapping machine and accelerometers were positioned on different positions on the floors and walls. The acceleration measurements were made using Integrated Circuit-Piezoelectric (ICP) accelerometers (50 g range, 100 mV/g general purpose accelerometer with 10-32 top connector and 10-32 mounting hole). Before each measurement, the entire arrangement was checked and calibrated.

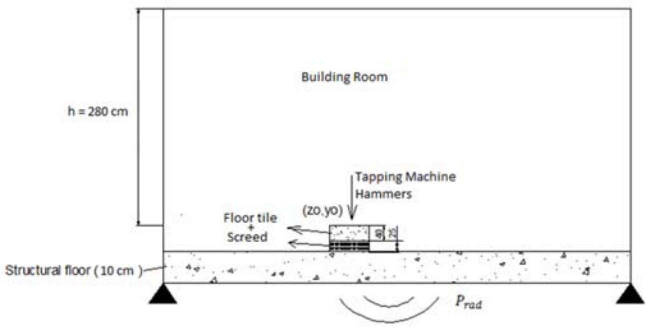

Fig. 1 Set-up of the experimental tests

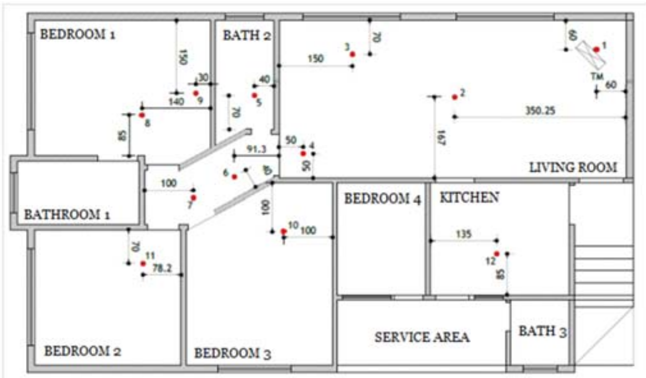

Fig. 2 Accelerometer positions on the apartment floor and tapping machine at position TM-1

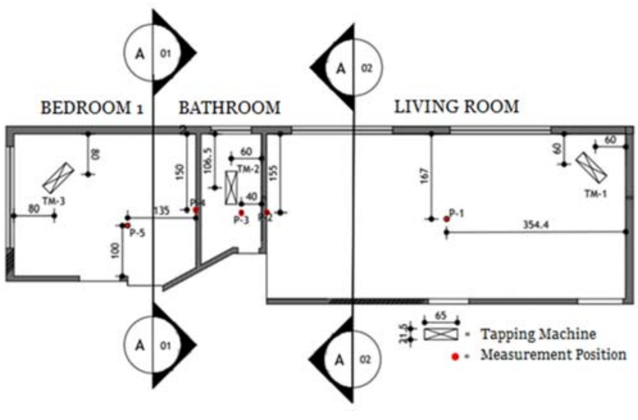

(a)

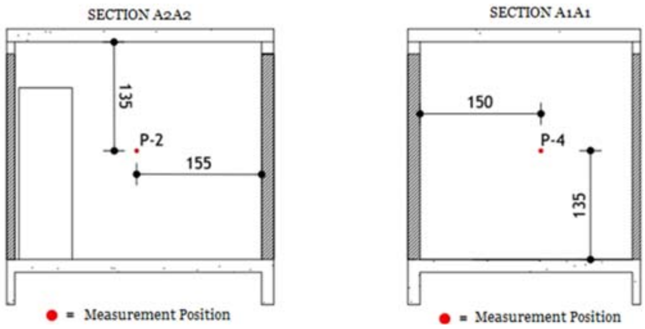

(b)

Fig. 3 Accelerometer and tapping machine positions on the apartment floor (P-1, P-3 and P-5) and walls (P-2 and P-4): (a) Floor plan; (b) Floor plan cuts (A_1 and A_2)

Next, the total loss factor of each floor and wall was measured indirectly using the structural reverberation time. Impulse responses were obtained using the impact testing procedure described as follows. On impacting the 'panel' by an instrumented hammer, the analyzer was triggered and started recording the response signal at the receiving point, where accelerometers were attached and connected to the acquisition equipment (National Instruments data acquisition module type NI-9234). The input signal was filtered by conveniently configuring the channel parameters. The acceleration levels were obtained via Fourier transforms of the measured quantities.

A frequency range of 100–4000 Hz was considered on measuring the acceleration levels due to the tapping machine. For the structural reverberation time, decay curves were measured in the frequency range 100-630 Hz, where the signal/noise ratio was high enough and the results were validated. The vibration source was a plastic headed hammer. It was used to hit the concrete panel at different locations (in order to obtain spatial averaged values) over a period of 6 seconds. The velocities were determined by integrating the accelerations at every frequency line.

III. Structural Reverberation Time

The structural reverberation time $\boldsymbol{T_s}$ was evaluated from the decay curves from a range of 5 dB to 25 dB below the steady-state level. Within the evaluation range a least-squares fit line was computed for the curve. The slope of the straight line gives the decay rate, *d*, in decibels per second, from which the structural reverberation time was calculated as $\boldsymbol{T_s} = 60/d$. The commercial software named WinMLS used the impulse responses for the calculation of the reverberation time.

The damping η, known as total loss factor, can be obtained using the equation:

$$\boldsymbol{\eta} = \frac{\mathbf{2.2}}{\boldsymbol{f\,T_s}} \tag{1}$$

where $\boldsymbol{T_s}$ is the structural reverberation time in seconds and $\boldsymbol{f}$ is the frequency in Hertz.

The values of damping η are sometimes termed structural damping, to identify that the damping is dependent on both the damping inherent in the material and that which comes from other mechanisms including dissipation losses at the boundary which might be significant. In other words, the total loss factor is equal to the sum of the internal loss factor of the material, the coupling loss factor to the adjacent structures and the radiation loss factor to the surrounding media [1].

An acquisition time of five seconds was adopted. Fig. 3 shows the accelerometer positions on the floors and walls for the reverberation time measurements. At very low frequencies, $\boldsymbol{T_s}$ depends to a large extent on the position of the source and the receiving accelerometer. It is recommended that an ensemble averaging procedure based on a combination of accelerometer positions be adopted for each one-third octave band result.

IV. Evaluation of the Vibration Reduction Index $\boldsymbol{K_{ij}}$

In this section the methodology used for the measurement of vibration reduction index $\boldsymbol{K_{ij}}$ of the cross-junction type is described. The vibration reduction index was obtained using the expression [4]:

$$\boldsymbol{K_{ij}} = \overline{\boldsymbol{D_{v,ij}}} + \boldsymbol{10log_{10}}\left(\frac{L_{ij}}{\sqrt{a_i a_j}}\right) \quad (2)$$

$$\overline{\boldsymbol{D_{v,ij}}} = \frac{D_{v,ij} - D_{v,ji}}{2} \quad (3)$$

$$\boldsymbol{a} = \frac{2.2\pi^2 S}{c_o T_s}\sqrt{\frac{f_{ref}}{f}} = \frac{\pi^2 S\eta}{c_o}\sqrt{\boldsymbol{f_{ref}f}} \quad (4)$$

where $\overline{\boldsymbol{D_{v,ij}}}$ is the average vibration level difference between the source element i and the receiving element j (walls, ceiling or floor); $\boldsymbol{L_{ij}}$ is the junction length between the source and the receiver; a is the equivalent absorption length; S is the area; $\boldsymbol{f_{ref}}$ is the reference frequency which is equal to 1,000 Hz; f is the center frequency; $\boldsymbol{c_o}$ is the sound phase speed in air and $\boldsymbol{\eta}$ is the total loss factor.

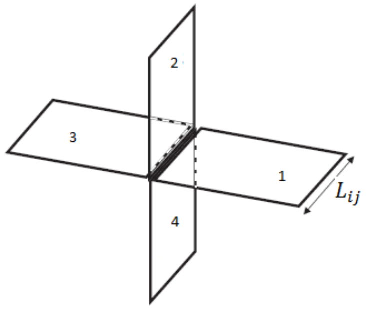

Fig. 4 Cross-junction type considered for the determination of the vibration reduction index K_{ij} between floors and walls: The subscripts i, j represent the source and receiver plate, respectively

The vibration source (tapping machine) was placed at particular positions in the building 2nd floor. The corresponding distances between the source and the receivers (accelerometers) are presented in Table I. The average vibration velocity level was then measured at points shown in Fig. 1. The first parameter to be measured was the vibration level in each 'subsystem' (floor and/or wall) which was the source or receiver plate (see Fig. 4). After that, the structural reverberation time was also measured.

V. Results and Discussions

Fig. 5 presents the time and space average acceleration levels of the floors. The variation of floor acceleration levels measured at different points is seen in Table I considering three distinct locations for the tapping machine: living room, bathroom and bedroom *1*. The values were obtained due to tapping machine generating impact vibrations and the corresponding accelerations being measured at points P_1, P_3 and P_5 (see Fig. 3 (a)). It is seen that the vibration level at point P_1 has the greatest values in the frequency range considered as the tapping machine was on the living room floor (Fig. 5 (a)). Likewise, the highest levels of acceleration at points P_3 and P_5 were for the tapping machine located on the bathroom floor and bedroom '1' respectively (see Figs. 5 (b) and (c)). It is also observed that the acceleration levels at distinct positions decrease as the distance from the tapping machine increases, as expected.

Fig. 6 presents the time average acceleration levels of two walls (points P_2 and P_4). It can be observed that the acceleration level varies according to the relative position between source (tapping machine) and receivers (accelerometers), as expected. It is seen that the highest vibration levels are found as the tapping machine was located on the bathroom floor which is supported on two of its edges by the corresponding walls.

TABLE I
Distances between the Sources (Tapping Machine at Position TM-1, TM-2 and TM-3) and the Receivers (Accelerometers at Positions P_1-P_5)

Distance Source/Receiver	P-1 cm	P-2 cm	P-3 cm	P-4 cm	P-5 cm
TM-1	313	656	706	795	938
TM-2	430	85	52	82	218
TM-3	780	426	358	288	176

In Fig. 7 it is seen that the vibrational level is dependent upon frequency and the distance between the source and receiver, as expected. In this case, the tapping machine is fixed at a particular position on the living room floor (see Fig. 2). There is a direct correlation between the distance between source-receiver and the acceleration level of the floors in most frequency range. Below 500 Hz, the acceleration levels vary as much as 40 dB. In general, structure-borne vibrational modes are predominant at frequencies below the critical frequencies of the floors. In this case, the critical frequency of the floors was approximately 185 Hz.

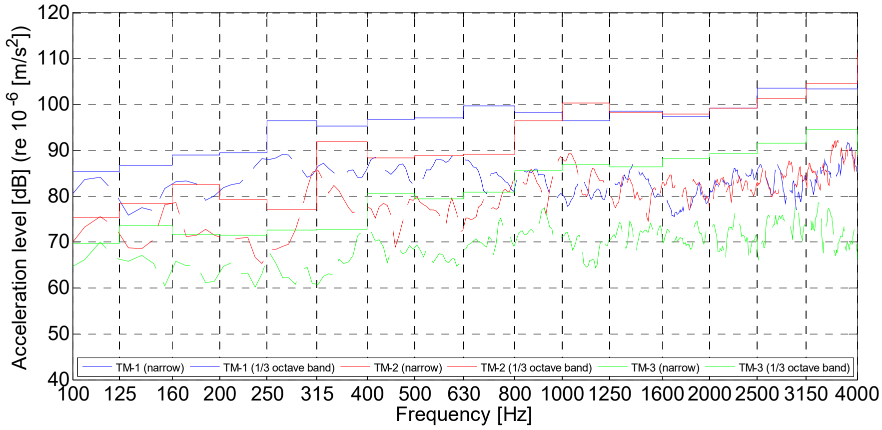

(a) Point P-1 (living room ceiling)

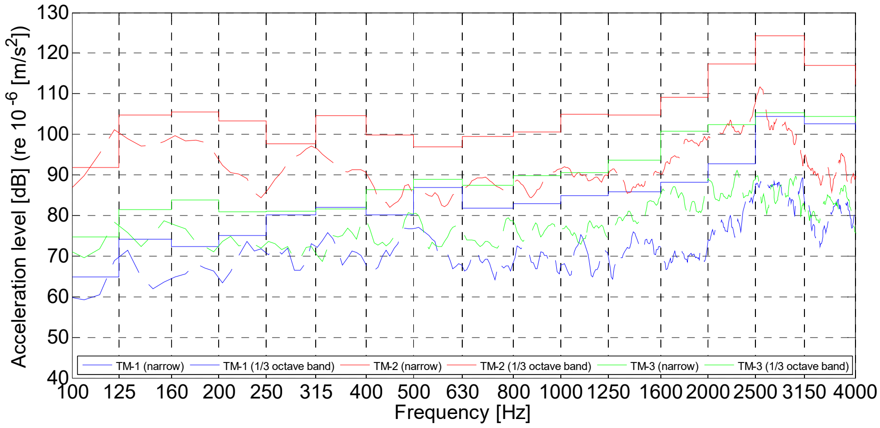

(b) Point P-3 (bathroom ceiling)

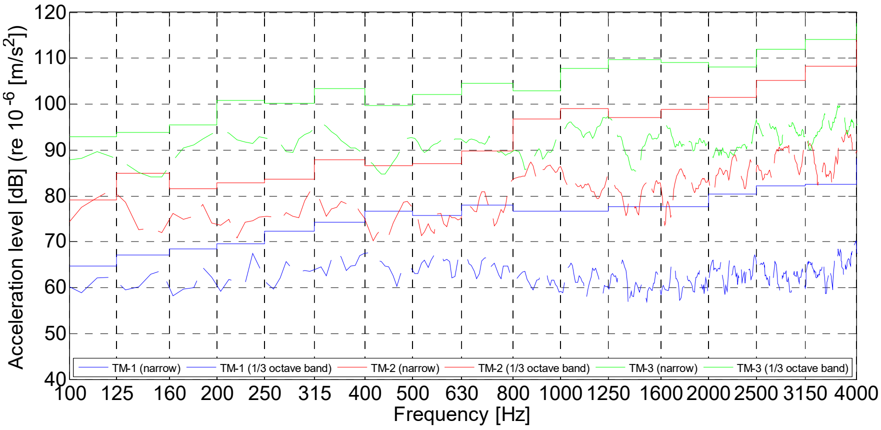

(c) Point P-5 (bedroom ceiling)

Fig. 5 Variation of floor acceleration level measured at distinct points considering the tapping machine location

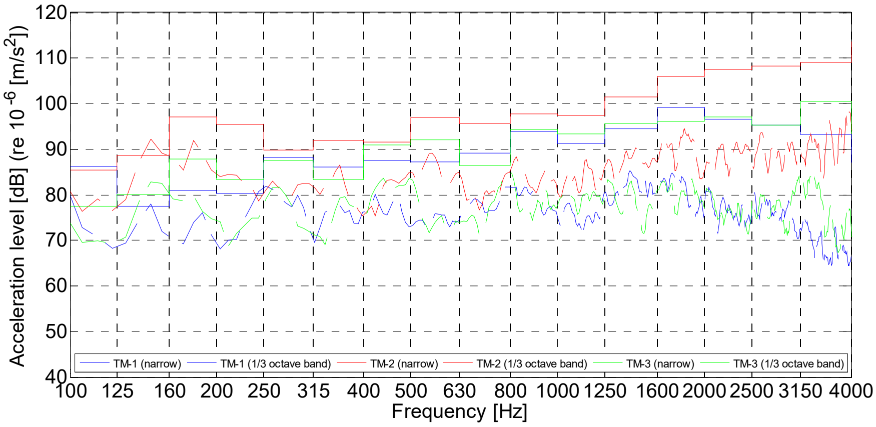

(a) Accelerometer on point P-2 (living room wall)

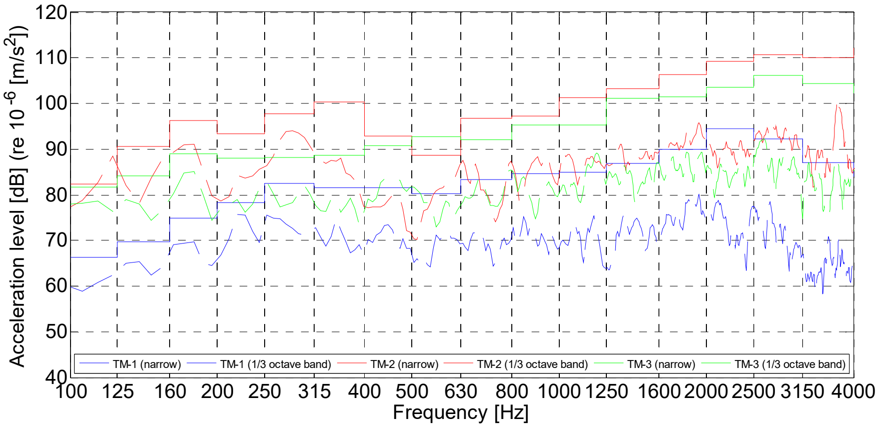

(b) Accelerometer on point P-4 (bedroom wall)

Fig. 6 Variation of wall acceleration level measured at distinct points considering the tapping machine location

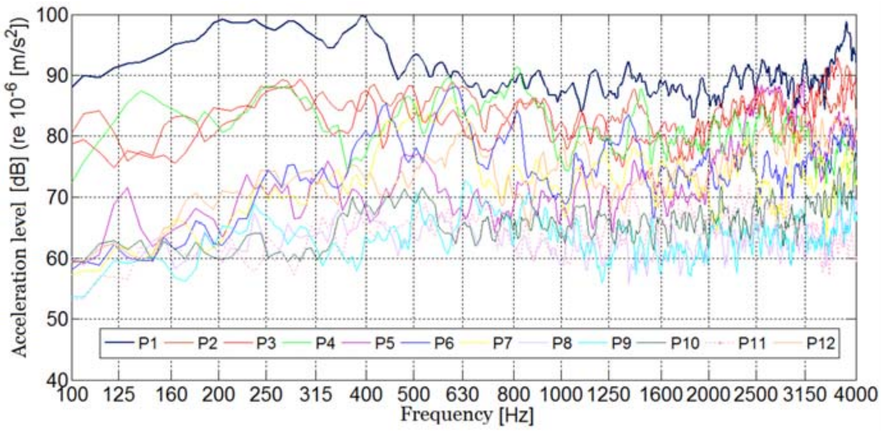

Fig. 7 Variation of floor acceleration level measured at distinct positions located in the apartment. The tapping machine location was fixed on the living room floor

TABLE II
STRUCTURAL REVERBERATION TIME OF FLOORS (ACCELEROMETERS AT POSITIONS P_1, P_3 AND P_5) AND WALLS (ACCELEROMETERS AT POSITIONS P_2 AND P_4)

1/3 octave band (Hz)	T_s(s) P-1	T_s(s) P-2	T_s(s) P-3	T_s(s) P-4	T_s(s) P-5
100	0.53	1.49	0.50	0.46	0.66
125	0.34	0.79	0.41	0.37	0.85
160	0.38	0.38	0.30	0.40	1.28
200	0.33	0.46	0.27	0.27	0.63
250	0.18	0.41	0.15	0.57	0.29
315	0.15	0.28	0.11	0.21	0.15
400	0.21	0.26	0.13	0.16	0.11
500	0.14	0.14	0.10	0.13	0.11
630	0.09	0.14	0.12	0.11	0.10

Table III shows the acceleration levels in 1/3 octave band center frequencies (dB re 10^{-6} m/s^2) measured at points $P_1 - P_5$ illustrated in Fig. 3. The level values are presented in the frequency range 100-630 Hz. These values were used in (2) and (3) for the determination of the vibration reduction index which are shown in Fig. 8.

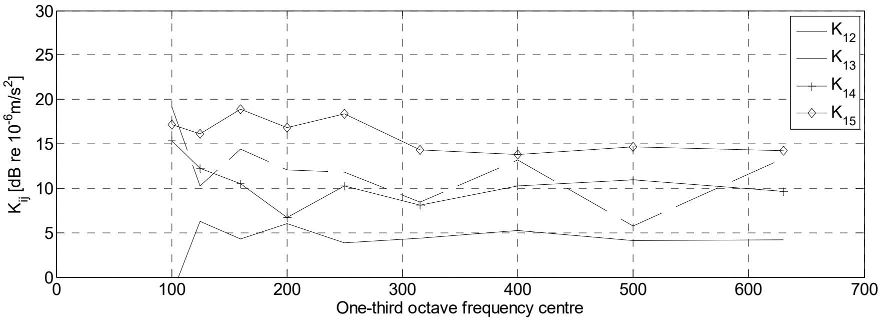

Fig. 8 Variation of the Vibration Reduction Index (K_{ij}) with frequency and accelerometer positions P_1 - P_5. Four different situations were considered: K_{12} (TM1 – P_2), K_{13} (TM1 – P_3), K_{14} (TM1 – P_4) and K_{15} (TM1 – P_5)

TABLE III
ACCELERATION LEVELS IN 1/3 OCTAVE BAND CENTER FREQUENCIES (DB RE 10^{-6} M/S^2) MEASURED AT POINTS $P_1 - P_5$ (SEE FIG. 3) AS THE TAPPING MACHINE CHANGE POSITIONS IN THE APARTMENT ROOMS (LIVING ROOM, BATHROOM AND BEDROOM 1)

Acceleration Level [dB re 10^{-6} m/s^2]/Freq. [Hz]	100 Hz	125 Hz	160 Hz	200 Hz	250 Hz	315 Hz	400 Hz	500 Hz	630 Hz
AL (TM-1, P_1)	85	86	89	90	96	95	97	97	99
AL (TM-2, P_1)	75	78	83	79	77	92	88	88	89
AL (TM-3, P_1)	69	73	72	72	73	73	81	79	81
AL (TM-1, P_2)	86	77	81	80	88	86	88	87	89
AL (TM-2, P_2)	85	89	97	95	89	92	92	97	96
AL (TM-3, P_2)	78	80	88	8	88	8	91	92	87
AL (TM-1, P_3)	65	74	72	75	80	82	80	87	81
AL (TM-2, P_3)	92	105	106	103	98	105	99	97	99
AL (TM-3, P_3)	75	81	84	81	81	82	86	89	87
AL (TM-1, P_4)	66	69	75	78	83	82	82	80	83
AL (TM-2, P_4)	82	91	96	93	98	100	93	89	96
AL (TM-3, P_4)	82	84	89	88	88	89	91	93	92
AL (TM-1, P_5)	65	67	68	70	72	74	77	76	78
AL (TM-2, P_5)	79	85	82	82	84	88	87	87	90
AL (TM-3, P_5)	93	94	95	101	100	104	99	102	105
Max	93	105.7	105.5	103.2	1002	104.7	99.9	102.2	104.5
Min	64,8	67,2	68.4	69.6	72.4	72.8	76.7	75.7	78.0
Avg	78,5	82,4	85,1	84,8	86,4	88,4	88,7	89,4	90,3
Var	84,9	96,1	114.1	101.9	80.7	93.9	49.3	52.8	59.3
Stdn	9.2	9.8	10.7	10.1	9.0	9.7	7.0	7.3	7.7

Fig. 8 shows the variation of K_{ij} with frequency. As expected, K_{15} and K_{12} show the top and bottom values in the whole frequency range. The difference between them reaches 15 dB in the frequency range. On the other hand, K_{13} and K_{14} present a difference of less than 5 dB between each other.

VI. CONCLUSIONS

The study presented herein is an alternative for understanding the structure-borne transmission across junctions in dwellings. Flanking transmission via flanked building floors and walls have been investigated using the concept of the parameter named vibration reduction index. This concept is a reliable approach which provides a rapid and practical measurement of the total sound power transmitted into structural panels. The method of measuring vibration acceleration levels, outlined in this study, is a cost-effective technique that can be used in place of traditional techniques which considers the structure sound radiation. In addition, experimental tests can be made in a noisier environment where background noise levels (measured in one octave band) can be tolerated. The acoustic-based technique may be alternatively applied to mechanical vibration techniques. The influence of vibration level exposure on the physiological and psychological behavior of humans inside residential buildings is already under investigation as part of future work.

ACKNOWLEDGMENTS

The author gratefully acknowledges the financial support provided by the Federal University of Minas Gerais (UFMG) and Cnpq (National Council for Scientific and Technological Development).

REFERENCES

[1] F. Fahy, *Sound and Structural Vibrations.* Academic Press, London, 1985.

[2] F. G. Leppington, E. G. Broadbent and K. H. Heron, The Acoustic Radiation Efficiency of Rectangular Panel. *Proceedings of the Royal Society of London. Series A, Math. and Physical Sciences,* 1982, 382, 245-271.

[3] M. D. C. Magalhaes and N. S. Ferguson, The development of a Component Mode Synthesis (CMS) model for three dimensional fluid-structure interaction, *J. Acoust. Soc. Am.* 2005, 118, 3679-3691.

[4] C. Hopkins, C. Crispim, J. Poblet-Puig and C. Guigou-Carter, Regression curves for vibration transmission across junctions of heavyweight walls and floors based on finite element methods and wave theory, *Applied Acoustics.* 2016, 113, 7-21.

[5] Rabold A.; Buschshmid, M.; Duster, A.; Muller, G.; Rank, E. Modelling the excitation force of a standard tapping machine on lightweight floor structures. *Building Acoustics*, 2010, vol 17, num 3, p. 175-197.

[6] Shi, W. Johansson, C., Sundback, U., An investigation of the characteristics of impact sound sources for impact sound insulation measurement. *Applied Acoustics*, 1997, v.51, 85-108.

[7] Shin, K., Park S., Kim, K. Sound prediction based on footstep-induced vibrations in concrete building using a convolutional neural network, *Applied Acoustics,* 2022, v. 198, p. 1-8.

[8] Schiavi, A., Astolfi, A., The prediction of the vibration reduction índex Kij for brick and concrete rigid junctions. *Applied Acoustics* 2010, 71, 523-530.